Pulmonary Artery Stiffness Is Independently Associated with Right Ventricular Mass and Function: A Cardiac MR Imaging Study[1]

Timothy J. W. Dawes, FRCA, PhD
Ajay Gandhi, MRCP
Antonio de Marvao, MRCP, PhD
Rui Buzaco, MD[2]
Paweł Tokarczuk, PhD
Marina Quinlan, BSc
Giuliana Durighel, MSc
Tamara Diamond, RN, BSc
Laura Monje Garcia, RN, MSc
Alain de Cesare, PhD
Stuart A. Cook, MRCP, PhD[3]
Declan P. O'Regan, FRCR, PhD

Purpose: To determine the relationship between pulmonary artery (PA) stiffness and both right ventricular (RV) mass and function with cardiac magnetic resonance (MR) imaging.

Materials and Methods: The study was approved by the local research ethics committee, and all participants gave written informed consent. Cardiac MR imaging was performed at 1.5 T in 156 healthy volunteers (63% women; age range, 19–61 years; mean age, 36.1 years). High-temporal-resolution phase-contrast imaging was performed in the main and right PAs. Pulmonary pulse wave velocity (PWV) was determined by the interval between arterial systolic upslopes. RV function was assessed with feature tracking to derive peak systolic strain and strain rate, as well as peak early-diastolic strain rate. RV volumes, ejection fraction (RVEF), and mass were measured from the cine images. The association of pulmonary PWV with RV function and mass was quantified with univariate linear regression. Interstudy repeatability was assessed with intraclass correlation.

Results: The repeatability coefficient for pulmonary PWV was 0.96. Increases in pulmonary PWV and RVEF were associated with increases in age ($r = 0.32$, $P < .001$ and $r = 0.18$, $P = .025$, respectively). After adjusting for age ($P = .090$), body surface area ($P = .073$), and sex ($P = .005$), pulmonary PWV demonstrated an independent positive association with RVEF ($r = 0.34$, $P = .026$). Significant associations were also seen with RV mass ($r = 0.41$, $P = .004$), RV radial strain ($r = 0.38$, $P = .022$), and strain rate ($r = 0.35$, $P = .002$), and independent negative associations were seen with radial ($r = 0.27$, $P = .003$), longitudinal ($r = 0.40$, $P = .007$), and circumferential ($r = 0.31$, $P = .005$) peak early-diastolic strain rate with the same covariates.

Conclusion: Pulmonary PWV is reliably assessed with cardiac MR imaging. In subjects with no known cardiovascular disease, increasing PA stiffness is associated with increasing age and is also moderately associated with both RV mass and function after controlling for age, body surface area, and sex.

Online supplemental material is available for this article.

[1] From the Medical Research Council Clinical Sciences Centre, Faculty of Medicine, Imperial College London, Hammersmith Hospital Campus, Du Cane Road, London, W12 0HS, England (T.J.W.D., A.d.M., R.B., P.T., M.Q., G.D., T.D., L.M.G., S.A.C., D.P.O'R.); Department of Cardiology, Imperial College NHS Healthcare Trust, London, England (A.G.); and Sorbonne Universités, UPMC Univ Paris 06, INSERM UMR_S 1146, CNRS UMR 7371, Lib, Paris, France (A.d.C.);
Received July 16, 2015; revision requested September 3; revision received October 26; accepted November 17; final version accepted November 24. Supported by the Medical Research Council, UK; National Institute for Health Research (NIHR) Biomedical Research Centre based at Imperial College Healthcare NHS Trust and Imperial College London, UK; NIHR Cardiovascular Biomedical Research Unit at Royal Brompton & Harefield NHS Foundation Trust and Imperial College London, UK; British Heart Foundation project grant (PG/12/27/29489). **Address correspondence to** D.P.O'R. (e-mail: *declan.oregan@imperial.ac.uk*).

[2] **Current address:** Department of Biomedical Sciences and Medicine, University of Algarve, Faro, Portugal.

[3] **Current address:** National Heart Centre Singapore, Singapore and Duke-NUS Graduate Medical School, Singapore.

This research was supported by by a Wellcome Trust-GSK fellowship grant.

One of the earliest manifestations of vascular aging in humans is impairment of central arterial function (1,2). Increased arterial stiffness in the systemic circulation is a strong predictor of cardiovascular events and all-cause mortality, which is related to both structural and functional differences of the left ventricle (LV) (3). While there is evidence that pulmonary arterial (PA) and aortic stiffness increase with age, it is not known whether the right ventricle (RV) adapts to aging in the same way as the LV does (1,2,4). This is clinically important because even mild RV hypertrophy is an independent predictor of heart failure and death in populations with no clinical cardiovascular disease at baseline (5).

Cardiac magnetic resonance (MR) imaging techniques for assessing the relationship between LV mass, contractile function, and aortic stiffness are well established, but applying them to the right side of the heart and pulmonary circulation is challenging because of the complex geometry of the RV and proximal branching of the PAs (6,7). High-temporal-resolution phase-contrast imaging has shown promise as a technique to overcome these limitations, allowing pulse wave velocity (PWV) to be measured in the pulmonary circulation; however, these methods have not been prospectively applied to cohort studies (8,9). Assessment of RV mass with cardiac MR imaging is a reproducible technique in healthy subjects, and recent advances in tissue-tracking technology now offer a powerful tool for assessing contractile function and diastolic relaxation in populations without RV hypertrophy (10–12). Our hypothesis was that, similar to the systemic circulation, age-related changes in PA stiffness are associated with prognostically adverse structural and functional adaptations in the RV. In this study, we set out to determine the relationship between PA stiffness and both RV mass and function by using cardiac MR imaging.

Advances in Knowledge

- Assessing pulmonary pulse wave velocity with cardiac MR imaging is a reliable (intraclass correlation coefficient, 0.96) way to noninvasively assess adaptations to aging in the cardiopulmonary system.
- Pulmonary artery stiffness increases with age ($r = 0.32$, $P < .001$) and is independently associated with both right ventricular mass ($r = 0.41$, $P = .004$) and diastolic relaxation ($r = 0.27$–0.40, all $P < .01$).

Materials and Methods

Study Population

All subjects provided written informed consent for participation in the study, which was approved by the local research ethics committee. Our prospective observational study included 156 healthy adult volunteers who were recruited by advertisement for a substudy of the United Kingdom Digital Heart Project. This cohort has no overlap with previously published data from this study (13,14). Healthy volunteers with no known cardiovascular disease were invited to participate by advertisement. In pre-enrolment screening, we excluded participants who were undergoing treatment for hypertension, diabetes, or hypercholesterolemia; with known occupational lung disease or pulmonary embolism; who were breast-feeding or pregnant; and who were taking prescription medication, with the exception of simple analgesics, antihistamines, and oral contraceptives. Standard safety contraindications to MR imaging were applied, including a weight limit of 120 kg.

MR Imaging Protocol

All images were acquired with a Philips 1.5-T MR Achieva system (Philips, Best, the Netherlands) by technologists (G.D., M.Q.) with at least 5 years of experience. The maximum gradient strength was 31 mT/m, and the maximum slew rate was 200 mT/m/msec. A 32-element cardiac phased-array coil was used for signal reception.

Ventricular function was assessed with standard balanced steady-state free precession cine images acquired in conventional cardiac short- and long-axis planes with the following typical parameters: repetition time msec/echo time msec, 3.2/1.6; voxel size, 1.5 × 1.5 × 8 mm; flip angle, 60°; sensitivity encoding factor, 2.0; bandwidth, 962 Hz/pixel; and temporal resolution, 29 msec (15). An additional RV long-axis image was acquired through the tricuspid annulus and the RV apex to assess longitudinal motion. Breath-holding pulmonary phase-contrast images were acquired perpendicular to the direction of flow in the main PA, 1 cm above the valve annulus, and in the right PA with the following sequence parameters: 3.9/2.3; voxel size, 1.4 × 1.4 × 10 mm; flip angle, 15°; sensitivity encoding factor, 2.0; bandwidth, 722 Hz/pixel; velocity encoding adjusted to avoid aliasing; and temporal

Implication for Patient Care

- Pulmonary artery stiffness should be evaluated as a potential contributory risk factor for cardiac dysfunction.

Published online before print
10.1148/radiol.2016151527 **Content codes:** CA MR

Radiology 2016; 280:398–404

Abbreviations:
CI = confidence interval
LV = left ventricle
PA = pulmonary artery
PWV = pulse wave velocity
RV = right ventricle
RVEF = RV ejection fraction

Author contributions:
Guarantors of integrity of entire study, T.J.W.D., A.G., M.Q., D.P.O'R.; study concepts/study design or data acquisition or data analysis/interpretation, all authors; manuscript drafting or manuscript revision for important intellectual content, all authors; approval of final version of submitted manuscript, all authors; agrees to ensure any questions related to the work are appropriately resolved, all authors; literature research, T.J.W.D., A.G., A.d.M., R.B., D.P.O'R.; clinical studies, T.J.W.D., A.G., A.d.M., R.B., M.Q., T.D., L.M.G., S.A.C., D.P.O'R.; experimental studies, A.G., R.B., M.Q., A.d.C., S.A.C.; statistical analysis, T.J.W.D., A.G., A.d.M., R.B., D.P.O'R.; and manuscript editing, T.J.W.D., A.G., A.d.M., R.B., M.Q., G..D., D.P.O'R.

Conflicts of interest are listed at the end of this article.

Figure 1

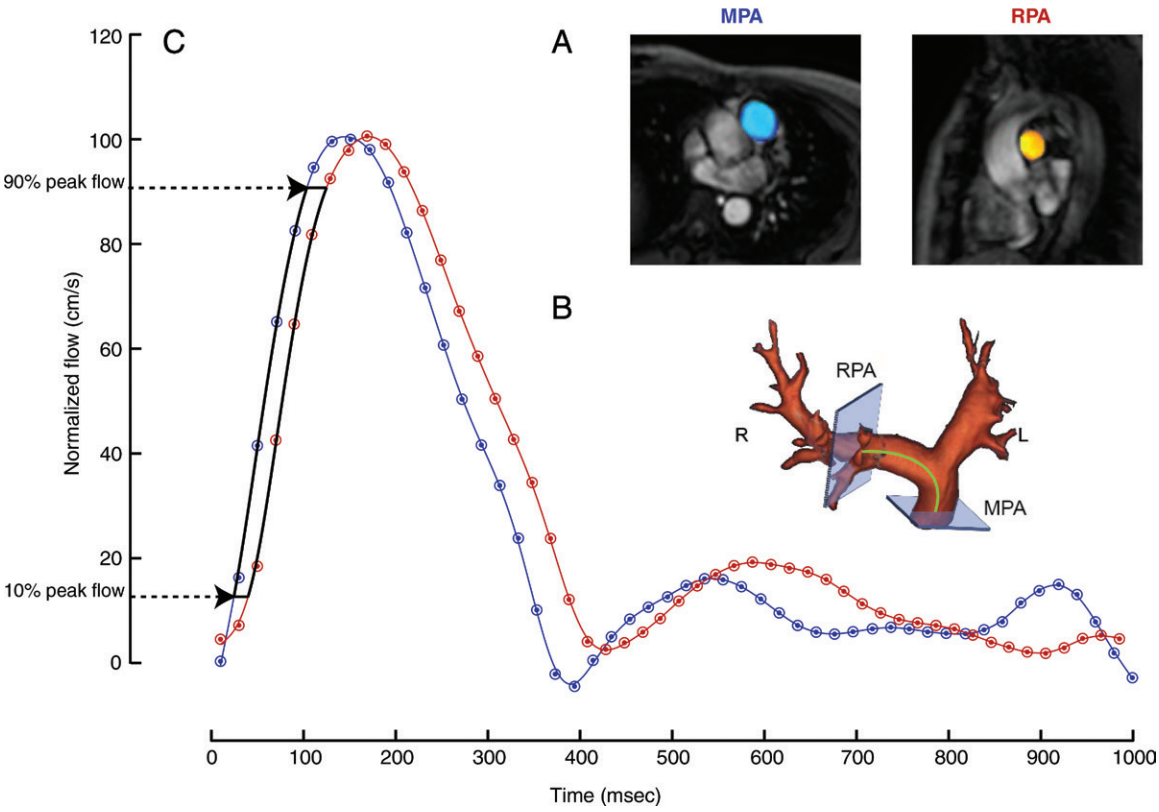

Figure 1: *A,* Phase-contrast MR images obtained in a 45-year-old woman show normalized flow waveforms in the main *(MPA)* and right *(RPA)* PAs. *B,* Pulmonary angiographic image shows the relationship of scanning planes and the path length (green line). *C,* Graph shows the transit time between the normalized flow waveforms, which was measured on the upslope of the curve between the points shown.

resolution, 15 msec. To calculate path length, a balanced steady-state free precession single shot sequence was performed by using a three-point plan along the main and right PAs intersecting the planes at which phase encoding was performed with the following parameters: 3.4/1.7; voxel size, 0.63 × 0.63 × 10 mm; flip angle, 60°; bandwidth, 722 Hz/pixel.

Pulmonary PWV Analysis

In each phase-encoded sequence, pulmonary PWV was calculated from the three-dimensional vessel length (D) and transit time (Δt) between the flow waveforms with validated software (ARTFUN; Inserm, Paris, France) (Fig 1) (6,16). On the magnitude phase-contrast images, regions of interest were drawn around the vessel lumen and automatically propagated through the cardiac cycle by two readers (A.G., with 2 years of MR imaging experience, and R.B., with 1 year of MR imaging experience). The path length was defined on anatomic images to create a three-dimensional Bezier curve through the center of the vessel that intersected the planes at which flow measurements were obtained. To minimize the variability of foot-to-foot measurement in the pulmonary system, the transit time was calculated as the average time difference between data points at 10%–90% of the normalized arterial systolic upslope with integration by parts between the flow curves. Pulmonary PWV was then calculated with the formula $D/\Delta t$.

Reliability

Repeatability was assessed in 20 consecutive subjects who were each imaged twice on the same day. Interobserver agreement was assessed by two independent readers (T.J.W.D., A.d.M.), each with 3 years of cardiac MR imaging experience.

RV Function Analysis

Cine image analysis was performed on a Philips ViewForum (Best, the Netherlands), and data were indexed to body surface area. Endocardial and epicardial borders of the RV were manually traced on short-axis cine images at end systole and end diastole by two reviewers (T.J.W.D., A.d.M.). The position of the pulmonary and tricuspid valves was referenced on long-axis images to ensure correct placement of the contours. Papillary muscles and trabeculae were included in the RV volumes but excluded from RV mass.

Systolic and diastolic function were quantified with feature-tracking software (TomTec Imaging Systems, Munich, Germany) and validated in both the RVs and LVs (11,12). Briefly, manual definition of an endocardial contour at end diastole by an observer (T.J.W.D.) served as an initialization from which software is used to track the displacement of spatial features in the time series of images (17). Systolic strain and strain rate, its temporal derivative, were measured in the RV from two- and four-chamber cine images (ie, longitudinal) and from short-axis cine images at the midpapillary level (ie, circumferential and radial) (Fig 2). For all measurements, the mean value across ventricular segments was calculated at each time point, and the peak value was recorded. For measurements that were recorded in more than one plane, peak values were averaged. Systolic and diastolic function were quantified by peak systolic strain and strain rate and by peak early diastolic strain rate, respectively. End diastole was identified as the frame with the largest end-diastolic area at the midpapillary level in the LV.

Statistical Analysis

Data were analyzed with R software, version 3.1.1 *(http://www.R-project.org)*. Preliminary associations were assessed with correlation analysis and simple linear regression. Multiple linear regression was used to assess for independent relationships after controlling for age, body surface area, and sex. Data were log-transformed to satisfy the assumptions of linear regression and tested by the normality of residuals (Shapiro-Wilk test), homoscedasticity (inspection of residual plots), and absence of multicollinearity (variance inflation factor) and outlier effects (Cook distance). All fields were centered and scaled before analysis to allow comparison of effect sizes. Continuous variables were compared between groups with the unpaired *t* test (two groups) or one-way analysis of variance (more than two groups) after logarithmic transformation, where necessary. Reliability was assessed with intraclass correlation coefficients.

Figure 2

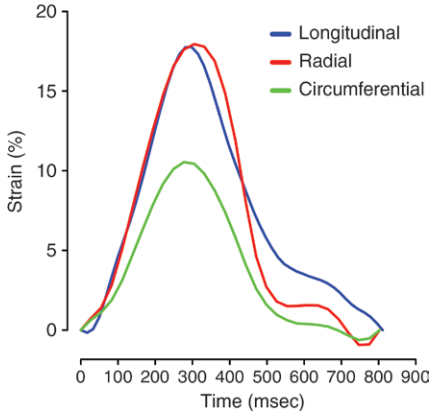

Figure 2: Graph shows examples of radial (red line), longitudinal (blue line), and circumferential (green line) strain obtained during the cardiac cycle in a 33-year-old woman with feature-tracking motion analysis.

Significance was assessed with two-tailed testing, with $P < .05$ indicating a significant difference.

Results

All 156 subjects completed the imaging protocol. All data sets were analyzed and included in the final analysis. Subjects' anthropometric data are described in the Table. The mean age of the cohort was 36.1 years (range, 19–61 years), and 63% were women. The difference in age between men and women was not significant (men: mean age, 34.6 years; standard error 1.1; age range, 22–55 years; women: mean age, 37.0 years; standard error 1.2; age range, 19–61 years; estimated difference between men and women, 2.4 years; 95% confidence interval [CI]: 0.7, 5.6 years, $P = .133$).

Reliability

Test-retest reproducibility and interobserver agreement are shown in Table E1 (online) for volumetry, PWV, and functional assessment. When pooling components of function, median absolute errors were higher for strain rate than they were for strain (intraobserver agreement, 13.9% vs 9.9% and $P = .027$; interobserver agreement, 14.9% vs 12.4% and $P = .328$; Wilcoxon rank sum test). When pooling strain and strain rate, mean absolute errors were similar for longitudinal, radial, and circumferential measures (intraobserver agreement, 8.1%, 14.6%, and 9.7%, respectively, and $P = .353$; interobserver agreement, 12.9%, 10%, and 19%, respectively, and $P = .608$; Kruskal-Wallis rank sum test).

Subject Characteristics and Cardiac MR Imaging–derived Measurements

Characteristic	Women	Men
Age (y)	37 (12)	35 (8)
Body surface area (m^2)	1.74 (0.16)	1.99 (0.17)
Indexed RV end-diastolic volume	86 (18)	98 (17)
Indexed RV end-systolic volume	41 (12)	52 (10)
Indexed RV mass	13 (5)	14 (5)
RVEF (%)	52 (9)	47 (8)
Pulmonary PWV (m/s)	2.2 (0.5)	2.2 (0.6)
Race*		
African-Caribbean	1 (0.6)	1 (0.6)
Black	3 (1.9)	2 (1.3)
Asian	7 (4.5)	11 (7.1)
White	80 (51.2)	42 (26.9)
Chinese	2 (1.3)	1 (0.6)
Mixed	5 (3.2)	1 (0.6)
Cigarette use*		
Yes	8 (5.1)	4 (2.6)
No	67 (42.9)	44 (28.2)
Unknown	0 (0)	1 (0.6)
Ex-smoker	23 (14.7)	9 (5.8)

Note.—Unless otherwise indicated, data are the mean, and data in parentheses are standard deviation. There were a total of 156 subjects, with 98 women and 58 men.

* Data are numbers of subjects, and data in parentheses are percentages.

Pulmonary PWV

There was no significant difference in pulmonary PWV between the sexes (women: mean, 2.19 m/sec; standard error, 0.05; men: mean, 2.21 m/sec; standard error, 0.07; mean difference, 0.019 m/sec; 95% CI: 0.162, 0.199; $P = .837$), races (mean difference, 0.009 m/sec; 95% CI: 0.129, 0.111; $P = .839$), and it was not associated with cardiac output ($r = 0.10$, $P = .224$). Pulmonary

Figure 3

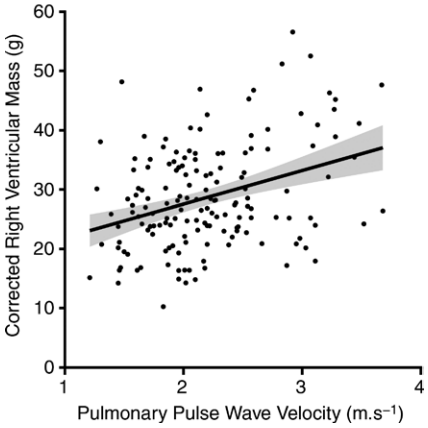

Figure 3: Scatterplot shows corrected RV mass (adjusted to mean age [36 years], body surface area [1.83 m^2], and female sex) versus pulmonary PWV, with regression line and 95% CI.

Figure 4

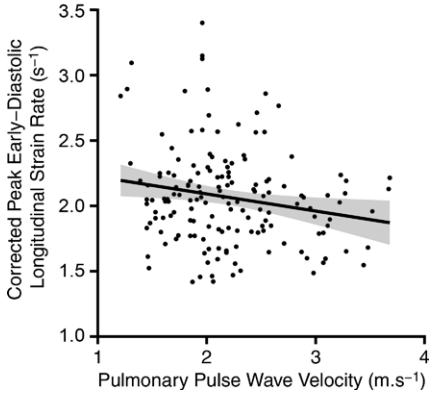

Figure 4: Scatterplot shows corrected peak end-diastolic longitudinal strain rate (adjusted to mean age [36 years], body surface area [1.83 m^2], and female sex) versus pulmonary PWV, with regression line and 95% CI.

PWV was significantly and positively associated with age ($r = 0.32$, $P < .001$).

RV Function

RV ejection fraction (RVEF) was significantly higher in women than in men (*t* test; mean RVEF, 52% vs 47%; $P < .001$), with no effect of race (analysis of variance, $P = .352$). Age was positively associated with RVEF ($r = 0.18$, $P = .025$) and negatively related to both RV end-systolic ($r = 0.27$, $P < .001$) and end-diastolic ($r = 0.22$, $P = .005$) volume. These associations persisted after adjustment for the effects of body surface area and sex (RVEF: $r = 0.31$ and $P = .022$; RV end-systolic volume: $r = 0.70$ and $P < .001$; RV end-diastolic volume: $r = 0.72$ and $P < .001$). RVEF was positively associated with LV ejection fraction ($r = 0.28$ and $P < .001$).

Pulmonary PWV and RV Function

Pulmonary PWV was positively associated with RVEF ($r = 0.34$, $P = .026$) after adjusting for age ($P = .090$), body surface area ($P = .073$), and sex ($P = .005$) and with RV mass ($r = 0.41$, $P = .004$) after adjusting for age ($P < .001$), body surface area ($P = .008$), and sex ($P = .086$) (Fig 3). PWV was associated with radial strain ($r = 0.17$, $P = .030$) and strain rate ($r = 0.25$, $P = .002$), but not with longitudinal strain ($r = 0.02$, $P = .802$), longitudinal strain rate ($r = 0.03$, $P = .688$), or circumferential strain ($r = 0.08$, $P = .334$). Circumferential strain rate showed a significant but weak negative association with pulmonary PWV ($r = 0.16$, $P = .043$). Pulmonary PWV was associated with significant and similarly sized reductions in radial, longitudinal, and circumferential peak early diastolic strain rate (Fig 4). All significant associations persisted after adjusting for age, body surface area, and sex (Table E2 [online]).

Discussion

In a large cohort of healthy adults, we found that PA stiffness increases with age and is independently associated with an increase in RV mass and diastolic stiffness after controlling for age, sex, and body surface area. These findings indicate that, similar to the systemic circulation, prognostically adverse changes in the RV are associated with vascular aging. Combined assessment of RV performance and PA stiffness with cardiac MR imaging provides a reliable means to evaluate physiologic adaptations of the cardiopulmonary unit.

Systemic arterial stiffness and wave reflection phenomena are recognized as important pathophysiologic mediators of the powerful contribution that arterial blood pressure has on cardiovascular risk (18). An association between LV hypertrophy and arterial stiffness is well documented in both adults and adolescents independent of blood pressure and is an established risk factor for cardiovascular events (19–21). Less is known about the effect of vascular aging on RV function and its impact on health outcomes, although echocardiographic estimates of PA pressure increase with age in the general population and are an indicator of all-cause mortality (4). Hemodynamic studies show that PA stiffness influences RV function, an effect that is mediated through changes in ventriculoarterial coupling (22–25). It is now recognized that, in adults without clinical cardiovascular disease at baseline, RV mass (measured with cardiac MR imaging) is an independent predictor of heart failure and cardiovascular death, even when accounting for variation in LV mass (5). It is not known what factors drive an increase in RV mass with age. Therefore, the aim of our study was to determine whether the relationship between vascular stiffness and myocardial hypertrophy seen in the systemic circulation is also present in the right side of the heart and PAs.

We showed that cardiac MR imaging offers reliable assessment of pulmonary PWV, RV mass, and RV strain in healthy volunteers by using measurements taken from phase-contrast images and feature tracking of balanced steady-state free precession cine images. In contrast to aortic PWV, there is a shorter path length in the pulmonary circulation over which to measure transit time, and there are distinct wave propagation and reflection effects (26). While free-breathing interleaved phase-contrast imaging has achieved a very high temporal resolution for measurement of PWV in the proximal PAs, a disadvantage is the long acquisition time and the potential for physiologic variation (8,9). We found that pulmonary PWV can be reliably assessed in healthy adults with the use of breath-hold phase-contrast

sequences performed with parallel imaging; however, greater improvements in spatial and temporal resolution may be achievable with techniques such as compressed sensing (27). Our data show that PA stiffness is positively associated with age, a finding consistent with experimental evidence that pulmonary vascular elastic properties decline over time, with an increase in medial thickness (28–30). We also observed that rising PA stiffness was moderately associated with both an increase in RV mass and a decline in diastolic function among apparently healthy adults. Age-related increases in RVEF were observed in other cohorts; because of the association with radial but not longitudinal or circumferential function, we suggest that this is principally related to an increase in radial contractility (31). Although a low pressure system makes distinctive demands on the right ventricle, our findings of an association between pulmonary vascular aging and increased RV mass and myocardial stiffness draw parallels with the physiologic characteristics of the systemic circulation (32). A tandem rise in vascular and ventricular stiffness occurs with aging in the aorta and LV associated with increasing afterload; our PWV and strain data show that a similar response may also occur in the PA and RV (33,34). How RV mass mediates cardiovascular risk in the general population is not known, but it was proposed that the RV serves as a more sensitive "barometer" of cumulative exposure to elevated LV end-diastolic pressure over time than a single measurement of LV mass or ejection fraction. Our data, supported by prognostic studies on PA pressure, and RV mass suggest that subclinical vascular aging may contribute to increasing afterload, RV hypertrophy, and diastolic dysfunction in the general population (4, 5).

The role of RV structure and function in both health and disease has historically been neglected compared with the epidemiologic characteristics of LV hypertrophy, systemic hypertension, and aortic aging, as is evidenced by the extensive literature on these topics. Our data shed light on the underlying pathophysiologic adaptations that occur in the cardiopulmonary unit of healthy subjects. There are alternatives to the use of cardiac MR imaging, since PA pressure can be estimated with echocardiography to measure tricuspid regurgitation velocity in the general population, but tricuspid regurgitation velocity is not assessable in 30% of subjects, and the range of PA pressure in the general population is relatively narrow (4,35). If the independent prognostic risk attributable to RV mass is mediated by a measurable change in pulmonary vascular function, it could prove to be a latent cardiovascular risk factor assessable only with cardiac MR imaging. If validated by longitudinal studies, pulmonary vascular function may be used to guide lifestyle modification or more intensive treatment of modifiable risk factors for heart failure.

Our study has limitations. A cross-sectional study cannot determine the causal relationship between increased PA stiffness and RV mass. We adjusted for age, sex, and body surface area, but other unmeasured factors, including LV end-diastolic pressure, may influence hemodynamics of the right side of the heart. For ethical reasons, we did not confirm normal PA pressure with catheterization of the right side of the heart, and we had no reference standard with which to compare cardiac MR imaging assessment of PWV. Transaxial imaging of the RV may provide easier identification of valve planes than the short axis, but volumetry is comparable in both axes in subjects without complex heart disease (36,37). Free-breathing interleaved phase-contrast sequences have achieved greater temporal resolution but require several minutes for acquisition, making them vulnerable to physiologic variations (9). The temporal resolution of our phase-contrast sequence was relatively low compared with the transit time being measured, but it achieved good repeatability in healthy adult subjects. Several authors have commented on the influence of reflection waves from short path lengths and frequent bifurcations (38,39). A "foot-to-foot" comparison of the flow curves would be appealing, as the effect of wave reflection would be minimal; however, as others have reported, this inflection point is indistinct in the pulmonary arteries (9). We used automated vessel tracking during the cardiac cycle but were not able to compensate for through-plane motion.

In conclusion, aging is related to increased PA stiffness in healthy adults and moderately associated with both RV mass and diastolic function. These findings suggest that prognostically adverse changes in RV function and morphologic features are associated with an age-related increase in PA stiffness.

Disclosures of Conflicts of Interest: T.J.W.D. disclosed no relevant relationships. **A.G.** disclosed no relevant relationships. **A.d.M.** disclosed no relevant relationships. **R.B.** disclosed no relevant relationships. **P.T.** disclosed no relevant relationships. **M.Q.** disclosed no relevant relationships. **G.D.** disclosed no relevant relationships. **T.D.** disclosed no relevant relationships. **L.M.G.** disclosed no relevant relationships. **A.d.C.** disclosed no relevant relationships. **S.A.C.** disclosed no relevant relationships. **D.P.O'R.** disclosed no relevant relationships.

References

1. Redheuil A, Yu WC, Mousseaux E, et al. Age-related changes in aortic arch geometry: relationship with proximal aortic function and left ventricular mass and remodeling. J Am Coll Cardiol 2011;58(12):1262–1270.
2. Cavalcante JL, Lima JA, Redheuil A, Al-Mallah MH. Aortic stiffness: current understanding and future directions. J Am Coll Cardiol 2011;57(14):1511–1522.
3. Vlachopoulos C, Aznaouridis K, Stefanadis C. Prediction of cardiovascular events and all-cause mortality with arterial stiffness: a systematic review and meta-analysis. J Am Coll Cardiol 2010;55(13):1318–1327.
4. Lam CS, Borlaug BA, Kane GC, Enders FT, Rodeheffer RJ, Redfield MM. Age-associated increases in pulmonary artery systolic pressure in the general population. Circulation 2009;119(20):2663–2670.
5. Kawut SM, Barr RG, Lima JA, et al. Right ventricular structure is associated with the risk of heart failure and cardiovascular death: the Multi-Ethnic Study of Atherosclerosis (MESA)--right ventricle study. Circulation 2012;126(14):1681–1688.
6. Dogui A, Redheuil A, Lefort M, et al. Measurement of aortic arch pulse wave velocity in cardiovascular MR: comparison of transit

time estimators and description of a new approach. J Magn Reson Imaging 2011;33(6):1321–1329.

7. Bell V, Sigurdsson S, Westenberg JJ, et al. Relations between aortic stiffness and left ventricular structure and function in older participants in the Age, Gene/Environment Susceptibility--Reykjavik Study. Circ Cardiovasc Imaging 2015;8(4):e003039.
8. Ibrahim SH, Shaffer JM, White RD. Assessment of pulmonary artery stiffness using velocity-encoding magnetic resonance imaging: evaluation of techniques. Magn Reson Imaging 2011;29(7):966–974.
9. Bradlow WM, Gatehouse PD, Hughes RL, et al. Assessing normal pulse wave velocity in the proximal pulmonary arteries using transit time: a feasibility, repeatability, and observer reproducibility study by cardiovascular magnetic resonance. J Magn Reson Imaging 2007;25(5):974–981.
10. Grothues F, Moon JC, Bellenger NG, Smith GS, Klein HU, Pennell DJ. Interstudy reproducibility of right ventricular volumes, function, and mass with cardiovascular magnetic resonance. Am Heart J 2004;147(2):218–223.
11. Hor KN, Gottliebson WM, Carson C, et al. Comparison of magnetic resonance feature tracking for strain calculation with harmonic phase imaging analysis. JACC Cardiovasc Imaging 2010;3(2):144–151.
12. Heermann P, Hedderich DM, Paul M, et al. Biventricular myocardial strain analysis in patients with arrhythmogenic right ventricular cardiomyopathy (ARVC) using cardiovascular magnetic resonance feature tracking. J Cardiovasc Magn Reson 2014;16:75.
13. Corden B, Keenan NG, de Marvao AS, et al. Body fat is associated with reduced aortic stiffness until middle age. Hypertension 2013;61(6):1322–1327.
14. de Marvao A, Dawes TJ, Shi W, et al. Population-based studies of myocardial hypertrophy: high resolution cardiovascular magnetic resonance atlases improve statistical power. J Cardiovasc Magn Reson 2014;16(1):16.
15. Kramer CM, Barkhausen J, Flamm SD, Kim RJ, Nagel E; Society for Cardiovascular Magnetic Resonance Board of Trustees Task Force on Standardized Protocols. Standardized cardiovascular magnetic resonance (CMR) protocols 2013 update. J Cardiovasc Magn Reson 2013;15:91.
16. Herment A, Mousseaux E, Jolivet O, et al. Improved estimation of velocity and flow rate using regularized three-point phase-contrast velocimetry. Magn Reson Med 2000;44(1):122–128.
17. Hor KN, Baumann R, Pedrizzetti G, et al. Magnetic resonance derived myocardial strain assessment using feature tracking. J Vis Exp 2011;(48):2356.
18. Safar ME, Levy BI, Struijker-Boudier H. Current perspectives on arterial stiffness and pulse pressure in hypertension and cardiovascular diseases. Circulation 2003;107(22):2864–2869.
19. Urbina EM, Dolan LM, McCoy CE, Khoury PR, Daniels SR, Kimball TR. Relationship between elevated arterial stiffness and increased left ventricular mass in adolescents and young adults. J Pediatr 2011;158(5):715–721.
20. Bluemke DA, Kronmal RA, Lima JA, et al. The relationship of left ventricular mass and geometry to incident cardiovascular events: the MESA (Multi-Ethnic Study of Atherosclerosis) study. J Am Coll Cardiol 2008;52(25):2148–2155.
21. Willum-Hansen T, Staessen JA, Torp-Pedersen C, et al. Prognostic value of aortic pulse wave velocity as index of arterial stiffness in the general population. Circulation 2006;113(5):664–670.
22. Milnor WR, Bergel DH, Bargainer JD. Hydraulic power associated with pulmonary blood flow and its relation to heart rate. Circ Res 1966;19(3):467–480.
23. Piene H, Sund T. Flow and power output of right ventricle facing load with variable input impedance. Am J Physiol 1979;237(2):H125–H130.
24. O'Rourke MF. Vascular impedance in studies of arterial and cardiac function. Physiol Rev 1982;62(2):570–623.
25. Piene H. Pulmonary arterial impedance and right ventricular function. Physiol Rev 1986;66(3):606–652.
26. Bouwmeester JC, Belenkie I, Shrive NG, Tyberg JV. Wave reflections in the pulmonary arteries analysed with the reservoir-wave model. J Physiol 2014;592(Pt 14):3053–3062.
27. Kwak Y, Nam S, Akçakaya M, et al. Accelerated aortic flow assessment with compressed sensing with and without use of the sparsity of the complex difference image. Magn Reson Med 2013;70(3):851–858.
28. Lankhaar JW, Westerhof N, Faes TJ, et al. Quantification of right ventricular afterload in patients with and without pulmonary hypertension. Am J Physiol Heart Circ Physiol 2006;291(4):H1731–H1737.
29. Ha B, Lucas CL, Henry GW, Frantz EG, Ferreiro JI, Wilcox BR. Effects of chronically elevated pulmonary arterial pressure and flow on right ventricular afterload. Am J Physiol 1994;267(1 Pt 2):H155–H165.
30. Pace JB. Sympathetic control of pulmonary vascular impedance in anesthetized dogs. Circ Res 1971;29(5):555–568.
31. Kawut SM, Lima JA, Barr RG, et al. Sex and race differences in right ventricular structure and function: the multi-ethnic study of atherosclerosis-right ventricle study. Circulation 2011;123(22):2542–2551.
32. Roman MJ, Ganau A, Saba PS, Pini R, Pickering TG, Devereux RB. Impact of arterial stiffening on left ventricular structure. Hypertension 2000;36(4):489–494.
33. Chen CH, Nakayama M, Nevo E, Fetics BJ, Maughan WL, Kass DA. Coupled systolic-ventricular and vascular stiffening with age: implications for pressure regulation and cardiac reserve in the elderly. J Am Coll Cardiol 1998;32(5):1221–1227.
34. Kang S, Fan HM, Li J, et al. Relationship of arterial stiffness and early mild diastolic heart failure in general middle and aged population. Eur Heart J 2010;31(22):2799–2807.
35. Gomberg-Maitland M. Something subtle about death: isolated systolic pulmonary pressure. Circulation 2009;119(20):2647–2649.
36. Schelhorn J, Neudorf U, Schemuth H, Nensa F, Nassenstein K, Schlosser TW. Volumetric measurements in patients with corrected tetralogy of Fallot: comparison of short-axis versus axial cardiac MRI and echocardiography [PubMed]. Acta Radiol 2015;56(11):1315–1322.
37. James SH, Wald R, Wintersperger BJ, et al. Accuracy of right and left ventricular functional assessment by short-axis vs axial cine steady-state free-precession magnetic resonance imaging: intrapatient correlation with main pulmonary artery and ascending aorta phase-contrast flow measurements. Can Assoc Radiol J 2013;64(3):213–219.
38. Hollander EH, Wang JJ, Dobson GM, Parker KH, Tyberg JV. Negative wave reflections in pulmonary arteries. Am J Physiol Heart Circ Physiol 2001;281(2):H895–H902.
39. Castelain V, Hervé P, Lecarpentier Y, Duroux P, Simonneau G, Chemla D. Pulmonary artery pulse pressure and wave reflection in chronic pulmonary thromboembolism and primary pulmonary hypertension. J Am Coll Cardiol 2001;37(4):1085–1092.